Free Radical Biology & Medicine 52 (2012) 2000–2012

Contents lists available at SciVerse ScienceDirect

Free Radical Biology & Medicine

journal homepage: www.elsevier.com/locate/freeradbiomed

Original Contribution

Oxidative protein folding and unfolded protein response elicit differing redox regulation in endoplasmic reticulum and cytosol of yeast

Marizela Delic [a], Corinna Rebnegger [a], Franziska Wanka [a], Verena Puxbaum [a,c], Christina Haberhauer-Troyer [b,c], Stephan Hann [b,c], Gunda Köllensperger [b,c], Diethard Mattanovich [a,c,*], Brigitte Gasser [a,c]

[a] Department of Biotechnology, University of Natural Resources and Life Sciences Vienna, 1190 Vienna, Austria
[b] Department of Chemistry, University of Natural Resources and Life Sciences Vienna, 1190 Vienna, Austria
[c] Austrian Centre of Industrial Biotechnology, 1190 Vienna, Austria

ARTICLE INFO

Article history:
Received 20 January 2012
Revised 24 February 2012
Accepted 24 February 2012
Available online 8 March 2012

Keywords:
UPR
Secretion
Glutathione
Redox-sensitive roGFP
Free radicals

ABSTRACT

Oxidative protein folding can exceed the cellular secretion machinery, inducing the unfolded protein response (UPR). Sustained endoplasmic reticulum (ER) stress leads to cell stress and disease, as described for Alzheimer, Parkinson, and diabetes mellitus, among others. It is currently assumed that the redox state of the ER is optimally balanced for formation of disulfide bonds using glutathione as the main redox buffer and that UPR causes a reduction of this organelle. The direct effect of oxidative protein folding in the ER, however, has not yet been dissected from UPR regulation. To measure in vivo redox conditions in the ER and cytosol of the yeast model organism *Pichia pastoris* we targeted redox-sensitive roGFP variants to the respective organelles. Thereby, we clearly demonstrate that induction of the UPR causes reduction of the cytosol in addition to ER reduction. Similarly, a more reduced redox state of the cytosol, but not of the ER, is observed during oxidative protein folding in the ER without UPR induction, as demonstrated by overexpressing genes of disulfide bond-rich secretory proteins such as porcine trypsinogen or protein disulfide isomerase (*PDI1*) and ER oxidase (*ERO1*). Cytosolic reduction seems not to be caused by the action of glutathione reductase (*GLR1*) and could not be compensated for by overexpression of cytosolic glutathione peroxidase (*GPX1*). Overexpression of *GPX1* and *PDI1* oxidizes the ER and increases the secretion of correctly folded proteins, demonstrating that oxidative protein folding per se is enhanced by a more oxidized ER and is counterbalanced by a more reduced cytosol. As the total glutathione concentration of these strains does not change significantly, but the ratio of GSH to GSSG is altered, either transport or redox signaling between the glutathione pools of ER and cytosol is assumed. These data clearly demonstrate that protein folding and ER stress have a severe impact on the cytosolic redox balance, which may be a major factor during development of folding-related diseases.

Protein folding and secretion can overburden the redox capacity of the endoplasmic reticulum (ER), with accumulation of reactive oxygen species (ROS) and misfolded or unfolded proteins in this compartment as a consequence. The cell reacts mostly with the activation of the unfolded protein response (UPR), triggering the transcription of a high number of genes involved in protein folding and the ER-associated degradation of the accumulated unfolded proteins [1,2].

ER stress as reaction to protein misfolding has been associated with various human diseases, such as Alzheimer, Parkinson, diabetes mellitus, atherosclerosis, and ischemia, as well as liver and heart diseases [3]. These pathologies may be linked to a disturbed glutathione metabolism as well [4]. The differentiation of B lymphocytes to plasma cells is also triggered by the interplay of UPR and redox signaling [5,6].

The oxidizing environment of the ER is well suited to the formation of disulfide bonds in proteins entering the secretory pathway. This highly organized cellular compartment contains a high number of chaperones and oxidoreductases assisting in the correct folding of proteins. The redox-active enzyme protein disulfide isomerase (Pdi) plays a crucial role in formation, isomerization, and reduction of disulfide bonds. During disulfide bond formation, Pdi accepts electrons from cysteine residues in nascent proteins, leading to the reduction of Pdi. Its FAD-dependent redox reaction partner enzyme Ero1 (ER oxidoreductin) interplays with Pdi1 during this process and passes the electrons to molecular oxygen (or other electron acceptors) to restore the oxidized form of Pdi1 [7]. This electron transfer cascade potentially leads to generation of ROS, a frequent source of oxidative stress and

* Corresponding author at: Department of Biotechnology, University of Natural Resources and Life Sciences Vienna, 1190 Vienna, Austria. Fax: +43 3697615.
E-mail address: diethard.mattanovich@boku.ac.at (D. Mattanovich).

0891-5849/$ – see front matter © 2012 Elsevier Inc. All rights reserved.
doi:10.1016/j.freeradbiomed.2012.02.048

damage in the cell. Glutathione, the main low-molecular-weight redox buffer, is a tripeptide with a pivotal role in bioreduction, protection against oxidative damage, detoxification from xenobiotics, and endogenous toxic metabolites [8]. In this respect, glutathione peroxidase (Gpx1) acts as a preventive antioxidant enzyme that is involved in the detoxification of ROS at the expense of reduced glutathione, whereas glutathione reductase (Glr1) is required for the recycling of the redox buffer [9]. Glutathione is present in the cell in both the reduced (GSH) and the oxidized form (GSSG) in different concentrations and ratios, depending on the cellular compartment. The GSH/GSSG ratio of the ER can range from 3/1 to 1/1 in mammalian microsomes, assuming the ER to be more oxidized than the cytosol [10,11]. Similar results were also achieved for yeast [12,13]. The more oxidizing ER environment is attributed both to a higher ratio of GSSG to GSH and to the activity of redox enzymes such as Pdi1 and Ero1.

As the UPR regulates numerous cellular processes it is difficult to discern between cellular reactions to protein folding kinetics, disulfide bond formation, glycosylation, and secretion organelle proliferation. For a clear investigation of oxidative protein folding a stringent discrimination between protein folding and UPR stress has to be observed. Yeast have been successfully applied as a model for protein folding and secretion, keeping the differences from higher eukaryotic cells in mind [14]. It should be noted that the secretion pathway of *Saccharomyces cerevisiae* differs significantly from that of higher eukaryotes and other yeasts, whereas that of *Pichia pastoris* better resembles that of mammalian cells [15]. As *P. pastoris* is well proven as a host for recombinant protein production, it is an ideal model for both eukaryotic cell physiology and biotechnological process development.

Although it is well established that the ER is a more oxidizing environment than the cytosol [10,16], in vivo measurement of the degree of oxidation in various compartments has become possible only with the development of redox-sensitive green fluorescent proteins (roGFPs) [13,17,18]. Thus it could be shown that the UPR leads to a reduction of the ER, whereas an effect on the cytosol has not been investigated so far.

Applying these redox-sensitive roGFPs we were able to dissect the effects of UPR from that of oxidative protein folding on the redox ratios of the cytosol and the ER of *P. pastoris*. Total concentrations of GSH and GSSG provided additional insights into cellular redox balance.

Material and methods

Strains and vectors

A summary of all strains used in this study is given in Table 1.

P. pastoris genes *ERO1* (PIPA00063), *PDI1* (PIPA01571), *GLR1* (PIPA03299), and *GPX1* (PIPA00848) were amplified from X-33 genomic DNA and cloned into a pPuzzle vector [19] under control of the GAP (glyceraldehyde-3-phosphate dehydrogenase) promoter; the zeocin resistance marker was flanked by loxP sites. The vector was integrated into the native gene locus of the *P. pastoris* genome after linearization in the respective sequence. After transformation by electroporation, positive transformants were selected on YPD plates with zeocin. Recycling of the marker was accomplished by transformation of the strains with a plasmid carrying the gene coding for the phage P1 Cre recombinase [20], thereby also generating strains containing just one copy of the respective target gene. The single-copy trypsinogen-expressing strain was produced similarly. For the localization of Gpx1, the gene was fused on its 3′ end with the sequence encoding the GluGlu epitope tag (EYMPME [21]) immediately preceding the stop codon. Vectors containing redox-sensitive GFP variants roGFP1 and roGFP1_iE for targeting the cytosol and the ER were described in [13] and were used for the transformation of the above-mentioned strains.

Cultivation conditions for redox and glutathione measurements

M2 minimal medium contained, per liter, 20 g of glucose, 20 g of citric acid, 3.15 g of $(NH_4)_2HPO_4$, 0.03 g of $CaCl_2 \cdot 2H_2O$, 0.8 g of KCl, 0.5 g of $MgSO_4 \cdot 7H_2O$, 2 ml of biotin (0.2 g L^{-1}), 1.5 ml of trace salts stock solution. The pH was set to 5.0 with 5 M KOH solution. Trace salts stock solution contained, per liter, 6.0 g of $CuSO_4 \cdot 5H_2O$, 0.08 g of NaI, 3.0 g of $MnSO_4 \cdot H_2O$, 0.2 g of $Na_2MoO_4 \cdot 2H_2O$, 0.02 g of H_3BO_3, 0.5 g of $CoCl_2$, 20.0 g of $ZnCl_2$, 5.0 g of $FeSO_4 \cdot 7H_2O$, and 5.0 ml of H_2SO_4 (95–98% w/w).

All analyzed clones were grown overnight in 5 ml M2 medium as preculture. Main cultures were inoculated to an OD_{600} 0.5 and incubated in 100-ml shake flasks at 28 °C at 170 rpm for 24 h. For each strain, 12 individual clones were used to inoculate 10 ml of medium.

Determination of redox ratios

Redox states of all strains were measured during the exponential growth phase. Total oxidation and reduction of the roGFPs were achieved by addition of 100 µl 6.3 mM 4,4′-dipyridyl disulfide and 200 µl 1 M dithiothreitol (DTT), respectively, and were compared to the untreated form. The fluorescence of the cells was detected in 96-well plates (FluoroNunc; Nunc) on a fluorescence photometer (Infinite M200 Tecan plate reader), on which it was possible to measure the excitation of two wavelengths, 395 and 465 nm, corresponding to the oxidized and the reduced form of the protein, and their emission at 530 nm. Each sample was measured four times [13]. To monitor whether there were any redox changes occurring during the measurement periods, samples were measured several times within 20 min at intervals of 5 min. In all cases, no significant changes in the redox ratio within these 20 min could be determined. Measurements of various dilutions of the cell suspensions were also calculated to have similar redox ratios. The degree of oxidation (OxD)

Table 1
Description of the strains used in this study.

Abbreviation	Description	Source
X-33	*Pichia pastoris* wild-type strain	Invitrogen
SMD1168H	Protease-deficient *P. pastoris* (*pep4*)	Invitrogen
HAC1	Wild type expressing the activated form of *Saccharomyces cerevisiae HAC1* under control of the GAP promoter	[24]
2F5 Fab	SMD1168 expressing the anti-HIV antibody 2F5 Fab fragment under control of the GAP promoter (production strain)	[52]
SMD trp	SMD1168 expressing porcine trypsinogen under control of the GAP promoter (production strain, more than one gene copy)	[53]
X-33 trp	X-33 expressing porcine trypsinogen under control of the GAP promoter (production strain, more than one gene copy)	
ERO1, PDI1, GPX1	X-33 wild-type strain transformed with an additional copy of *ERO1, PDI1,* or *GPX1* under control of the GAP promoter	[13], this study
trp	X-33 wild-type strain transformed with a plasmid carrying the gene coding for porcine trypsinogen	This study
ERO1trp, PDI1trp, GPX1trp	Trypsinogen-producing strain (trp) transformed with an additional copy of *ERO1, PDI1,* or *GPX1*	This study
PDI1trp multi	Trypsinogen-producing strain (trp) transformed with two additional copies of *PDI1*	This study
PDI1/GPX1trp multi	Trypsinogen-producing strain (trp) transformed with an additional copy of *PDI1* and three additional copies of *GPX1*	This study
PDI1/GPX1trp	Trypsinogen-producing strain (trp) transformed with an additional copy each of *PDI1* and *GPX1*	This study

of the cytosol and the ER was calculated according to the following equation:

$$OxD = \left(\frac{R - R_{red}}{\frac{I465_{ox}}{I465_{red}}(R_{ox} - R) + (R - R_{red})} \right).$$

The quotient of fluorescence intensities, $I465_{ox}/I465_{red}$, is the so-called "instrument factor" and corrects for variations in the signal strength from the instrument. R is the experimentally determined fluorescence ratio of the intensities for the two wavelengths 395 and 465 nm [22]. R_{ox} and R_{red} stand for the ratios of fully oxidized or fully reduced roGFP, whereas R is the ratio of the untreated sample.

Determination of glutathione concentration by liquid chromatography–tandem mass spectrometry (LC/MS-MS)

Five milliliters of the M2 minimal medium served as preculture and was inoculated with the strains and incubated overnight at 28 °C. Ten milliliters of the same medium was then inoculated with an OD_{600} of 0.5 of each strain and incubated for 24 h at 28 °C and 170 rpm (exponential growth phase). The pellet of 1 ml of this culture in three replicates was collected by centrifugation at 3000 rpm for 5 min at 4 °C. The cells were resuspended in 1 ml ice-cold 0.1 M H_3PO_4, spiked with labeled glutathione–glycine–$^{13}C_2$,^{15}N (Sigma–Aldrich) and GSSG–glutathione–glycine–$^{13}C_2$,^{15}N (synthesized in house), and heated to 75 °C for 3 min to extract GSH and GSSG. The cell extracts were measured by LC/MS-MS (Agilent ion trap) using hydrophilic interaction chromatography and acetonitrile/water as eluent (C. Haberhauer-Troyer et al., submitted for publication). Oxidation of GSH to GSSG during sample preparation was controlled to avoid formation of GSSG artifacts. For this purpose the formation of mixed (labeled/unlabeled) disulfide was monitored as an indicator of oxidation.

Total cell extracts from S. cerevisiae (BY4741) and P. pastoris (X-33, PDI1)

One milliliter of the overnight culture (in YPD) of all strains (OD_{600} 15) was centrifuged and the supernatant was discarded. Cell pellets were resuspended in 500 µl resuspension buffer containing 20 ml phosphate-buffered saline (PBS), 1% Triton X-100, and protease inhibitor (Sigma). Two hundred fifty microliters of acid-washed glass beads was added to each cell suspension. Mechanical cell disruption was performed in the MP Biomedicals Fast Prep: 3 × 20 s at 6 m/s. SDS (0.5%) was added and the cell extracts were boiled for 5 min at 99 °C. Total protein amount was determined with the BCA assay (Thermo Fisher Scientific).

SDS–polyacrylamide gel electrophoresis (PAGE) and Western blot

Supernatant samples (trypsinogen) or cell extracts (Pdi1) were analyzed by 12% SDS–PAGE (NuPAGE Novex Bis-Tris; Invitrogen) under denaturing conditions according to the manufacturer's instructions. For the detection of Pdi1, the gels were electroblotted onto a nitrocellulose membrane, which was treated with a 1:1000 dilution of mouse anti-PDI (ab4644; Abcam) or mouse anti-HDEL antibody (sc-53472; Santa Cruz Biotechnology) in PBS with 0.1% Tween and 2% bovine serum albumin (BSA). The secondary antibody was a 1:10,000 dilution of anti-mouse antibody conjugated with alkaline phosphatase (A3438; Sigma) in PBS with 0.1% Tween and 2% BSA. Protein bands of Western blots were visualized with the Conjugate AP Substrate kit (Bio-Rad).

Isolation of total RNA from P. pastoris, reverse transcription of mRNA and determination of transcript levels by quantitative real-time PCR

RNA isolation, cDNA synthesis, and measurement of mRNA transcript levels using real-time PCR were performed as described in [19]. Actin was used as reference gene for normalization. Each gene was correlated to actin as an internal control, and the untreated wild-type strain X-33 served as the reference strain for each relative transcript level determination using the $\Delta\Delta C_t$ method. Primers are given in the supplementary material (Table S3).

Production of porcine trypsinogen

Screening medium contained, per liter, 10 g pea peptone, 10 g yeast extract, 10.2 g $(NH)_2HPO_4$, 1.24 g KCl, 910 µl 1 M $CaCl_2$ solution, and 1 ml biotin stock solution (0.2 g/L). All analyzed clones were inoculated in 5 ml YPD medium as preculture. For the main culture, cells were grown in 100-ml shake flasks incubating at 28 °C at 170 rpm for 48 h. Ten individual clones were used to inoculate 10 ml of medium. The amount of secreted trypsinogen was determined in the supernatant by measuring the activity of trypsin, the activated form. The sample buffer was exchanged to 1 mM HCl over PD-10 columns (Amersham Biosciences). Then, 50 µl of sample was incubated with 5 µg bovine enterokinase (Sigma) in 50 mM Tris–HCl buffer, pH 8.6, containing 50 mM $CaCl_2$, to activate the trypsinogen, and finally the activity was determined using the *p*-toluene sulfonyl-L-arginine ethyl ester–HCl (TAME) assay. Aliquots of the samples were added to 40 mM Tris–HCl buffer, pH 8.1, containing 10 mM $CaCl_2$ and 1 mM TAME, and the increase in absorbance at 247 nm was followed. Trypsinogen concentration was calculated using the specific activity coefficient $\varepsilon = 0.0101\ E_{247}\ cm^{-1}\ min^{-1}$ for 1 µg/mL trypsin [23].

Staining of ROS

The fluorescent probes DHE (dihydroethidium), DHR (dihydrorhodamine 123), and DCF (2′,7′-dichlorodihydrofluorescein diacetate) were used to determine the levels of ROS. DHE and DHR were added to cells at a final concentration of 10 µg/ml, and DCF was diluted to a final concentration of 40 µg/ml in PBS. Cells at an OD_{600} of 0.4 were harvested by centrifugation and resuspended in 2 ml PBS. In the following the cells were treated with the three fluorescent dyes and incubated at 30 °C for 30 min. Flow cytometry analysis was performed using a FACS Canto with the settings DHR and DCF green filter (525–550 nm), DHE red filter (600–650 nm).

Fluorescence microscopy

The strains were cultivated as described for redox and glutathione measurements. After 24 h of cultivation the cells were either viewed directly or stained for vacuole and nucleus detection.

Vacuoles were stained using FM4-64 (Molecular Probes). A 15 µM solution was prepared by diluting a 1.6 mM solution in culture medium. The cells were harvested (700 *g*, 3 min) and resuspended at OD_{600} 15 per milliliter in 15 µM FM4-64 solution. After 15 min incubation at 30 °C the solution was replaced by fresh medium and the cells were incubated for another hour with shaking at 30 °C. Finally the cells were harvested, resuspended at OD_{600} 15 per milliliter in fresh medium, and viewed under the microscope.

Staining of the nuclei was achieved by fixing the cells in 1 ml 4% formaldehyde (Thermo Scientific) in PBS with 1 mM $MgCl_2$ and mixing end-over-end at room temperature for 1 h. After being washed twice with PBS, the cells were finally resuspended in 300 µl PBS. Three microliters of the suspension was placed on a Polysine slide (Thermo Scientific) and mixed with 3 µl Vectashield mounting medium (Vector Laboratories) containing 50 ng/ml DAPI (Invitrogen).

Finally a coverslip was added and the cells were viewed under the microscope.

The cells were viewed on a Leica DMI 6000 fluorescence microscope equipped with an HCX PL Apo 100× 1.40 NA oil-immersion objective, a Leica CCD camera, and appropriate bandpass filters to detect GFP, DAPI, and FM4-64. At all times a differential interference contrast (DIC) image was taken as well. ImageJ was used for brightness and contrast adjustments and for performing the merged images.

Untransformed wild-type strains were used as negative controls. Images were taken and processed based on the controls, which showed no visible signal.

Immunofluorescence microscopy

Yeast strains were grown in minimal medium for 24 h with a final OD_{600} of 0.25–1.0. Eight milliliters of the culture was filtered using a bottle-top filter (Whatman). The cells on the filter were resuspended in 5 ml of 4% formaldehyde in PBS + 1 mM $MgCl_2$ and transferred to a 15-ml Falcon tube. After incubating end-over-end for 1 h at room temperature the cells were centrifuged for 3 min at 890×*g* in a low-speed centrifuge. The cells were washed twice with 5 ml of 100 mM potassium phosphate buffer (pH 6.5) + 1 mM $MgCl_2$ and resuspended in yeast-staining sorbitol buffer (YSSB; 100 mM potassium phosphate, 0.9 M sorbitol) to a final OD_{600} of 10. One hundred microliters of cell suspension was transferred to a 1.5-ml microcentrifuge tube and 0.6 µl of 2-mercaptoethanol and 5 U of lyticase were added. After incubating for 30 min at 30 °C, the spheroplasts were centrifuged for 3 min at 500×*g* in a microcentrifuge, gently resuspended in 500 µl of YSSB, washed once more with 500 µl of YSSB, centrifuged, and finally resuspended in 100 µl YSSB. Thirty microliters of this spheroplast suspension was added to each well of a poly-L-lysine (0.01%; Sigma)-coated IBIDI 15 µ-Chamber 12-well glass slide and incubated for 10 min at room temperature in a humid chamber. Excess liquid was blotted off with a cotton swab and 100 µl of ice-cold methanol was added to each well of the dried glass slide. After 5 min the methanol was removed and the glass slide was left to dry. Three hundred microliters of freshly made blocking solution (PBS, pH 7.4, 1% dried milk, 0.1% bovine serum albumin, 0.1% Triton X-100) was added to each well and incubated overnight at 4 °C in a humid chamber. The blocking solution was removed and 100 µl of primary antibody solution was added (purified mouse monoclonal anti-GluGlu; Covance; diluted 1:100 in blocking buffer). The slide was incubated for 1 h in a humid chamber followed by washing the wells six times with 300 µl of blocking buffer. Now 100 µl of secondary antibody solution (Alexa Fluor 488 donkey anti-mouse IgG (H + L) or Alexa Fluor 555 goat anti-mouse IgG (H + L); Molecular Probes; diluted 1:100 in blocking buffer) was added to the respective wells. After 1 h incubation in the dark, again each well was washed six times with blocking buffer and once with PBS. Finally, the slide chamber was removed and 5 µl of Vectashield mounting medium was added to each sample. For DAPI staining, 5 µl of Vectashield supplemented with 50 ng/ml DAPI was added to the samples. A coverslip was placed onto the slide and sealed with nail polish. The cells were viewed on a Leica DMI 6000 SP5 confocal microscope using an HCX PL Apo 63.0× 1.30 NA glycerin-immersion objective and 405, 488, and 561 nm lasers. For DAPI and Alexa Fluor 555 images, sequential scans were performed [54,55].

Statistical analyses

To visualize the means and variability of roGFP data, they are represented as box-and-whisker plots. Each box is separated into two interquartiles by the statistical median as a horizontal line in the box. The extreme values extending from the interquartile at most 1.5 times from the upper or lower interquartile are the whiskers. Points at a greater distance from the median than 1.5 represent potential outliers.

Secreted trypsinogen labels and glutathione concentrations are expressed as the mean ± standard error of the mean. Differences between groups were tested using Student's *t* test. All strains were compared to the wild-type strain X-33 or the single-copy trypsinogen secreting strain.

Results

Induction of the UPR leads to significant reduction of the redox ratios in both the ER and the cytosol

Recently, we established and described a method for measuring the intracellular redox conditions of various cellular compartments in living yeast cells [13]. To study the relationship between protein folding in the ER lumen, oxidative stress, and the redox environment in the ER and cytosol, we analyzed the impact on the cellular redox pool. As model systems we selected *P. pastoris* strains secreting two different classes of disulfide-containing proteins, which rely on correct disulfide bond formation for their activity or dimerization, respectively. Porcine trypsinogen is a pancreatic enzyme containing six disulfide bonds, whereas the human antibody Fab fragment 2F5 contains five disulfide bonds, one thereof required to connect the heavy chain–light chain dimer. Secretion levels were determined to be ~290 µg 2F5 Fab/g wet cell weight (wcw) and ~388 µg trypsinogen/g wcw in shake-flask cultivations. These strains were transformed with the redox-sensitive biosensors roGFP1 and roGFP1_iE, respectively, and compared to their wild-type strain.

The secretion of the model protein trypsinogen caused a reduction of both the ER and the cytosol, compared to the wild-type strains X-33 and SMD 1168H, whereas the production of the 2F5 Fab fragment led to a slight reduction of the ER and a significant reduction of the cytosol (Figs. 1A and B). Transcript analysis of UPR target genes (*PDI1, ERO1, KAR2)* revealed that the UPR was induced in all strains (see Supplementary Fig. S1).

To distinguish if the reduction of both compartments is due to protein secretion or caused by UPR induction, we analyzed a strain with a constitutively activated UPR [24]. The redox ratios of a *P. pastoris* strain overexpressing the activated form of the UPR transcription factor *HAC1* was measured as described above. Induction of several UPR target genes (*KAR2, PDI1, ERO1*) is shown in Supplementary Fig. S1.

Similar to the results obtained by chemical UPR induction [12], overproduction of the transcription factor Hac1p led to a reduction of the ER (Fig. 1C), resulting in a calculated reduction potential of $E'_{hc} = -248$ mV for this organelle (compared to −242 mV for the wild type). As already shown for the recombinant-protein-secreting strains, *HAC1* overexpression also had a significant impact on the redox state of the cytosol (Fig. 1D), leading to a reduction of this compartment as well ($E'_{hc} = -315$ mV vs −303 mV in the wild type). Reduction of the cytosol was rather unexpected as UPR induction led to the formation of ROS, as shown in Supplementary Fig. S2. Notably, both hydrogen peroxide (reported as a consequence of increased Ero1 activity [25]) and superoxide anion (as described in [26] during ER stress) were detected.

Fluorescence microscopy was applied to verify the correct localization of the two redox sensors in X-33 wild-type and Hac1-overproducing strains. As expected, in both strains roGFP1 was found in the cytosol and roGFP1_iE was targeted to the ER, indicated by the characteristic circular structure (Fig. 2A). DAPI staining confirmed the perinuclear ER pattern of roGFP1_iE (Fig. 2B, top two rows), whereas staining of the vacuolar membrane with FM4-64 visually separates vacuole and cytosol, demonstrating the localization of roGFP1 in the cytosol (Fig. 2B, bottom two rows). These results clearly show that UPR induction did not influence the localization of roGFP1 or roGFP1_iE.

As Hac1 has been shown to regulate the expression of more than 1000 genes in *P. pastoris* during UPR activation [24], it was not clear whether the observed changes in the redox ratios display an effect

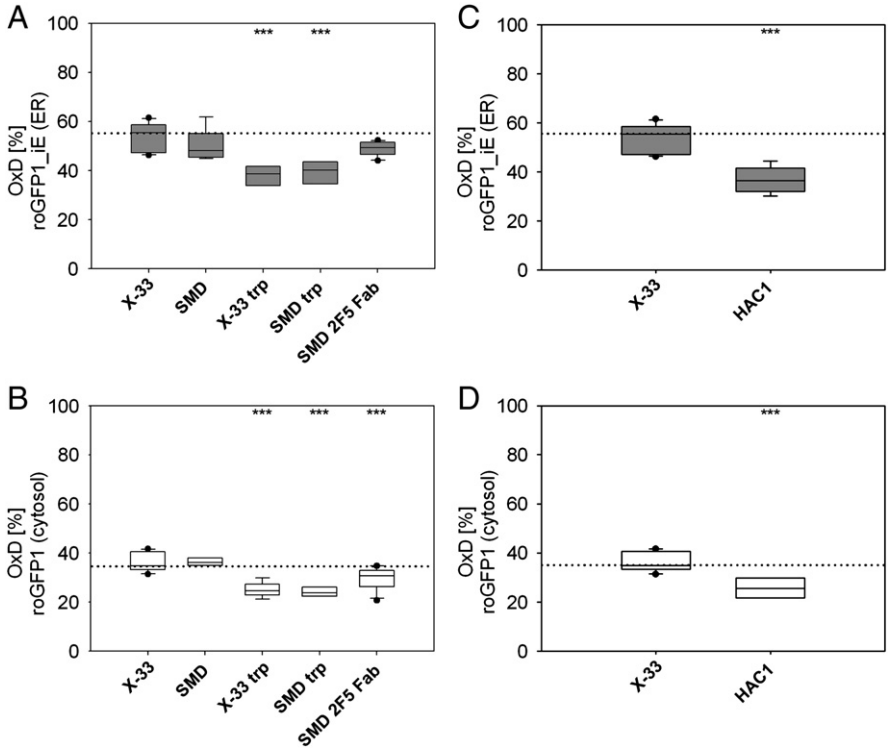

Fig. 1. UPR induction leads to a reduction of the redox ratios in both the ER and the cytosol. *P. pastoris* wild-type strains (X-33 and SMD1168H), strains secreting either porcine trypsinogen or antibody 2F5 Fab fragment, and a strain overexpressing *S. cerevisiae HAC1* were transformed with the redox-sensitive biosensors roGFP1_iE and roGFP1. ***$p<0.01$ according to Student's *t* test. (A) ER redox ratios of the wild-type strains X-33 and SMD1168H and strains overexpressing trypsinogen or 2F5 Fab fragment. (B) Cytosolic redox ratios of strains X-33 and SMD1168H and strains overexpressing trypsinogen or 2F5 Fab fragment. (C) ER redox ratios of wild-type strain X-33 and X-33 overexpressing the UPR transcription factor *HAC1*. (D) Cytosolic redox ratios of wild-type strain X-33 and X-33 overexpressing the UPR transcription factor *HAC1*.

caused by protein folding or if they are the consequence of other reactions activated by the UPR. To be able to dissect the effects of folding and secretion on the redox ratios of the different compartments from effects caused by UPR induction, we set out to investigate a strain producing a secretory protein that did not lead to UPR activation.

Production of recombinant secretory proteins without UPR induction significantly reduces the cytosol, but does not influence ER redox status

Porcine trypsinogen was chosen for this purpose, as secretion of Fab fragments activated the UPR in all investigated strains, whereas UPR induction with trypsinogen was dependent on its gene copy number. Therefore, we generated a strain containing a single copy of the trypsinogen (pTRP) expression cassette without a marker gene by using the Cre/lox system [20,27]. Quantitative real-time PCR of *ERO1*, *PDI1*, and *KAR2* transcript levels was performed to verify that UPR was not induced (Fig. 3A). Additionally, no production of ROS was detected in this single-copy trypsinogen-secreting strain (Fig. 3B). Secretion levels of trypsinogen were 38 μg/g wcw. This strain was further transformed with the roGFPs for redox studies.

Without triggering ER stress, production of trypsinogen did not change the redox status of the ER (Fig. 3C); however, it still caused a significant reduction in the redox ratio of the cytosol (Fig. 3D). This reaction seems to be specific for recombinant secretory proteins, as production of a recombinant cytosolic protein did not lead to redox changes in the two compartments (data not shown).

Increased transcript levels of PDI1 and ERO1 lead to reduction of the cytosol, but only PDI1 causes oxidation of the ER redox state

As Ero1 and Pdi1 are the main players of the oxidative protein folding machinery in the ER, we measured the impact of their overexpression on the redox ratios of the cytosol and the ER. An additional copy of these two genes was introduced into the *P. pastoris* genome under control of the strong and constitutive GAP promoter, either alone or in combination. Transcript levels of the target genes, as well as *KAR2* and glutathione-related genes (*GLR1*, *GPX1*, and *GSH1*), were determined using quantitative real-time PCR (Fig. 4A). Compared to the wild type, mRNA levels were enhanced in the overexpressing strains: 17-fold for *ERO1* and 13-fold for *PDI1* overexpression. No cross-regulation between the individual genes was observed. Furthermore, no induction of the UPR target gene *KAR2* or the amount of the protein was observed, confirming that UPR was not activated in the strains. Growth was similar to the wild type for all strains. Exemplarily, the amount of Pdi1 increased in the *PDI1*-overexpressing strain compared to the wild type. Because of the lack of specific antibodies against *P. pastoris* proteins, we used the anti-HDEL antibody, as Pdi1 is an ER-resident protein that carries a C-terminal HDEL retention signal. With the Western blot, it could be clearly demonstrated that *PDI1* overexpression led to significantly higher amounts of Pdi1 protein compared to its wild-type strain (Fig. 4G).

Changes in the redox ratio of the ER and the cytosol were analyzed in both the wild-type strain X-33 and the trypsinogen-producing strain overexpressing these genes (Figs. 4B and C). Very low impact on the ER redox potential was observed in the *ERO1*-overexpressing strains (Fig. 4B). The overexpression of *PDI1* showed that the ER can undergo further oxidation, as we have reported previously [13], which is more significant in the trypsinogen-secreting strain. Furthermore, the coexpression of *PDI1* with trypsinogen led to formation of ROS (Fig. 4D), which was not observed upon *ERO1* coexpression or *PDI1* overexpression in the wild-type strain (Fig. 4E). Thus, Pdi1 activity seems to be increased by the presence of higher levels of its substrates, in this case the recombinant secretory protein trypsinogen. *PDI1* overexpression also led to more than twofold higher titers of active trypsinogen in the culture supernatant (Fig. 4B, black bars). The combination of *PDI1* and *ERO1* overexpression in one strain resembled the PDI1trp

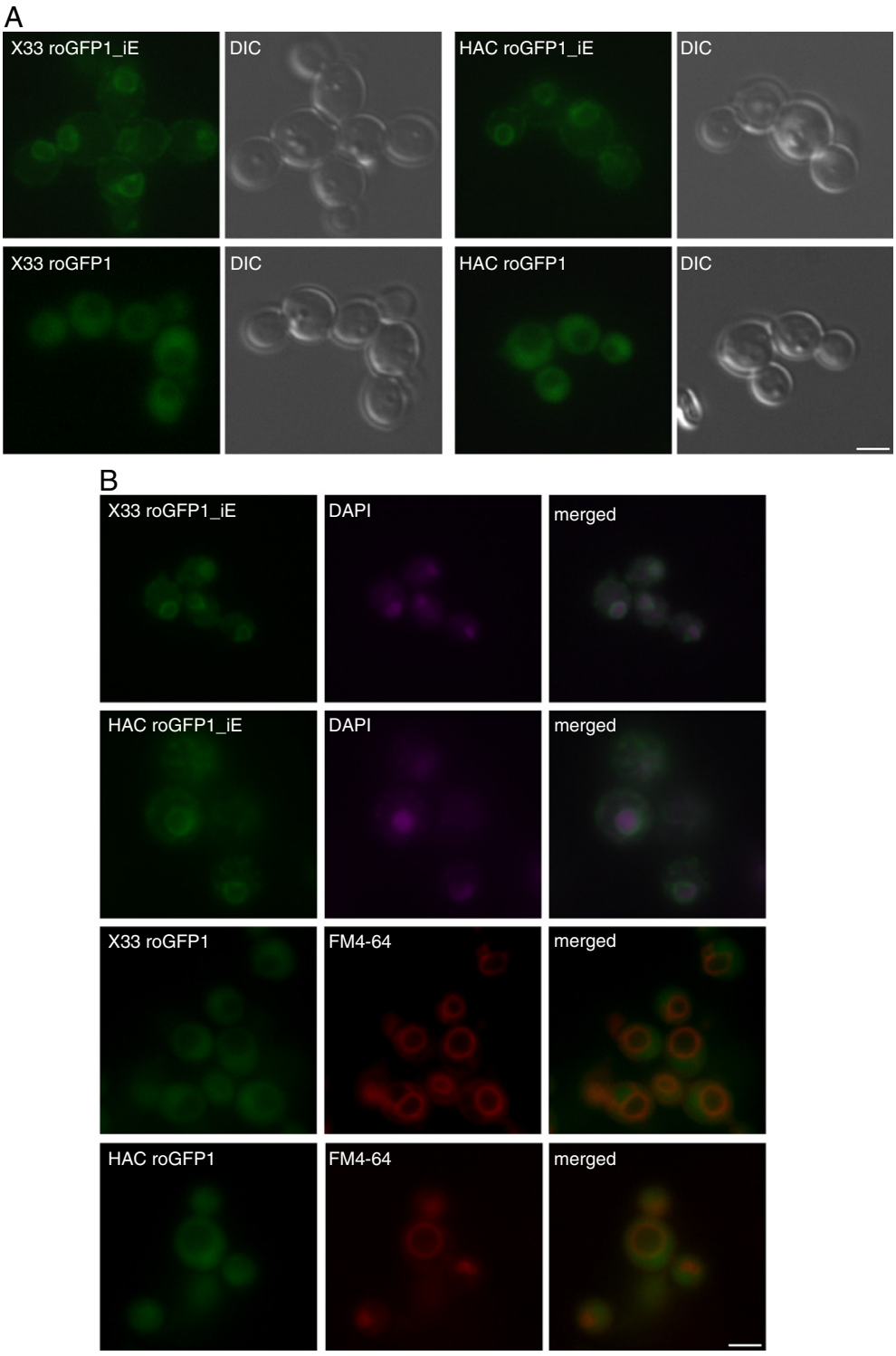

Fig. 2. Subcellular localization of roGFP1 and roGFP1_iE in wild-type X-33 and Hac1-overproducing strains. (A) Fluorescence images of X-33 wild-type (left) and Hac1-overproducing strains (right) expressing roGFP1_iE (top) and roGFP1 (bottom). DIC images of all samples were taken at the same time. (B) Top two rows: X-33 wild-type and Hac1-overproducing strains expressing roGFP1_iE were stained with DAPI (purple). Images of DAPI and GFP were taken and the fluorescence images were overlaid. (Bottom two rows) X-33 wild-type and Hac1-overproducing strains expressing roGFP1 were stained with FM4-64 (red). Images of GFP and FM4-64 were taken and the fluorescence images were overlaid. Scale bar, 3 μm.

phenotype regarding the redox ratios and the amount of secreted trypsinogen (data not shown).

Furthermore, it could be clearly demonstrated that overproduction of the two ER-resident proteins, Ero1 and Pdi1, had an impact on the redox state of the cytosol, once more leading to a reduction of this cellular compartment (Fig. 4C). This is in accordance with the results obtained for trypsinogen, thus indicating that oxidative folding of disulfide bond-rich secretory proteins in the ER has a strong impact on the cytosol.

As roGFPs are described to react predominantly with glutathione, this implicates a cross talk between cytosolic and ER glutathione redox pools upon oxidative protein folding.

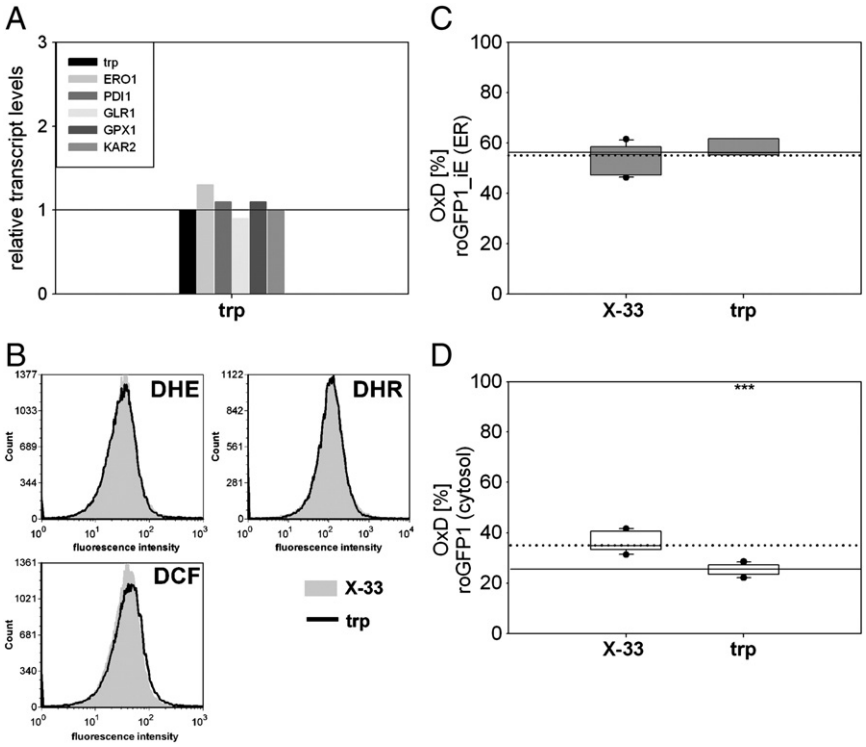

Fig. 3. Folding and secretion of a disulfide-rich protein causes reduction of the cytosol, but not the ER. Wild-type strain X-33 and a trypsinogen-secreting strain with a single trp gene copy were transformed with the redox sensors roGFP1_iE and roGFP1. (A) Transcript levels of the genes *ERO1, PDI1, GLR1, GPX1,* and *KAR2* measured by quantitative real-time PCR. (B) The strains X-33 and trp, stained with DHE, DHR, and DCF for ROS and measurement by flow cytometry. (C) ER redox ratios of the strains X-33 and trp. (D) Cytosolic redox ratios of the strains X-33 and trp.

Co-overexpression of GPX1 with a disulfide-rich secretory protein leads to oxidation of the ER and reduction of the cytosol, whereas GLR1 co-overexpression affects only the ER redox state

Glutathione reductase is a key enzyme in the conversion of oxidized GSSG to its reduced form GSH and is crucial for the maintenance of the cellular glutathione redox potential. Glutathione peroxidase, on the other hand, is an enzyme involved in the detoxification of ROS, in particular H_2O_2, at the expense of reduced glutathione, thereby generating GSSG. The impact of these two enzymes on the cytosol and the ER redox potential was evaluated in the wild-type and the trypsinogen-producing strains to find out if higher expression levels of these two enzymes involved in glutathione metabolism influenced the phenotype observed above.

Strains overexpressing these genes under control of the GAP promoter were analyzed with the ER and cytosol-targeted roGFPs (Figs. 5A and B). Transcript levels were enhanced 37-fold for *GPX1* and 39-fold for *GLR1* overexpression. No cross-regulation between the individual genes was observed. Furthermore, no induction of the UPR target genes *ERO1, KAR2,* and *PDI1* was seen, confirming that UPR was not activated (Fig. 5C).

Overproduction of Glr1, a protein that has been described to be localized to both cytosol and mitochondria in *P. pastoris* [28], did not influence the cytosolic redox state, but led to a significant reduction of the ER (Figs. 5A and B). Gpx1 overproduction on the other hand caused a reduction of the cytosol (Fig. 5B), as did Ero1 and Pdi1 (Fig. 4C).

Strikingly, overproduction of Gpx1, which is presumably localized in the cytosol based on bioinformatics prediction [29], caused a further oxidation of the ER when co-overexpressed with trypsinogen (Fig. 5A), as already seen for *PDI1* overexpression (Fig. 4B). Once again, the level of secreted trypsinogen was enhanced (~1.6-fold) in conjunction with a more oxidizing ER environment (Fig. 5A, black bars). To exclude the possibility that the effect of *GPX1* overexpression on the ER is due to the localization of Gpx1 within this compartment, we marked the protein with a GluGlu epitope tag on its C-terminus and analyzed its cellular localization with immunofluorescence staining and confocal laser scanning microscopy. As can be seen in Fig. 5D, no perinuclear staining (indicative for ER) was detected using an anti-GluGlu epitope antibody, confirming that Gpx1 is not targeted to the ER. In addition to cytosolic staining of Gpx1, some punctate structures are visible within the cells, which may be an indication of additional mitochondrial localization, as has been recently observed for a *S. cerevisiae* Gpx isoform [30]. Localization of Gpx1 was identical in the wild type and in the trp background overexpressing the GluGlu-tagged protein. Exemplarily, the images of the GPX1trp strain are shown, as the redox effect on the ER was more pronounced in this strain.

Combined overexpression of PDI1 and GPX1 leads to a further oxidation of the ER

With the intention to investigate whether further oxidation of the ER is possible, or if Gpx1 is able to rescue the *PDI1* phenotype regarding its cytosolic redox potential, we co-overexpressed *PDI1* and *GPX1* together in the trypsinogen-secreting strain. As shown in Fig. 6A, the combination of *PDI1* and *GPX1* resulted in a further oxidation of the ER. Moreover, when either *GPX1* or *PDI1* was present in more than one gene copy, an additional increase in the oxidation status of this compartment could be monitored. Again, a correlation of trypsinogen secretion levels (black bars in Fig. 6A) with the ER redox states was observed, which raises the hypothesis that a more oxidizing ER environment promotes the secretion of (recombinant) proteins.

Regarding the cytosol, the redox ratios of the *PDI1/GPX1* co-overexpressing clones were less reduced than their respective parental trypsinogen-expressing strain, declining to the conditions observed in

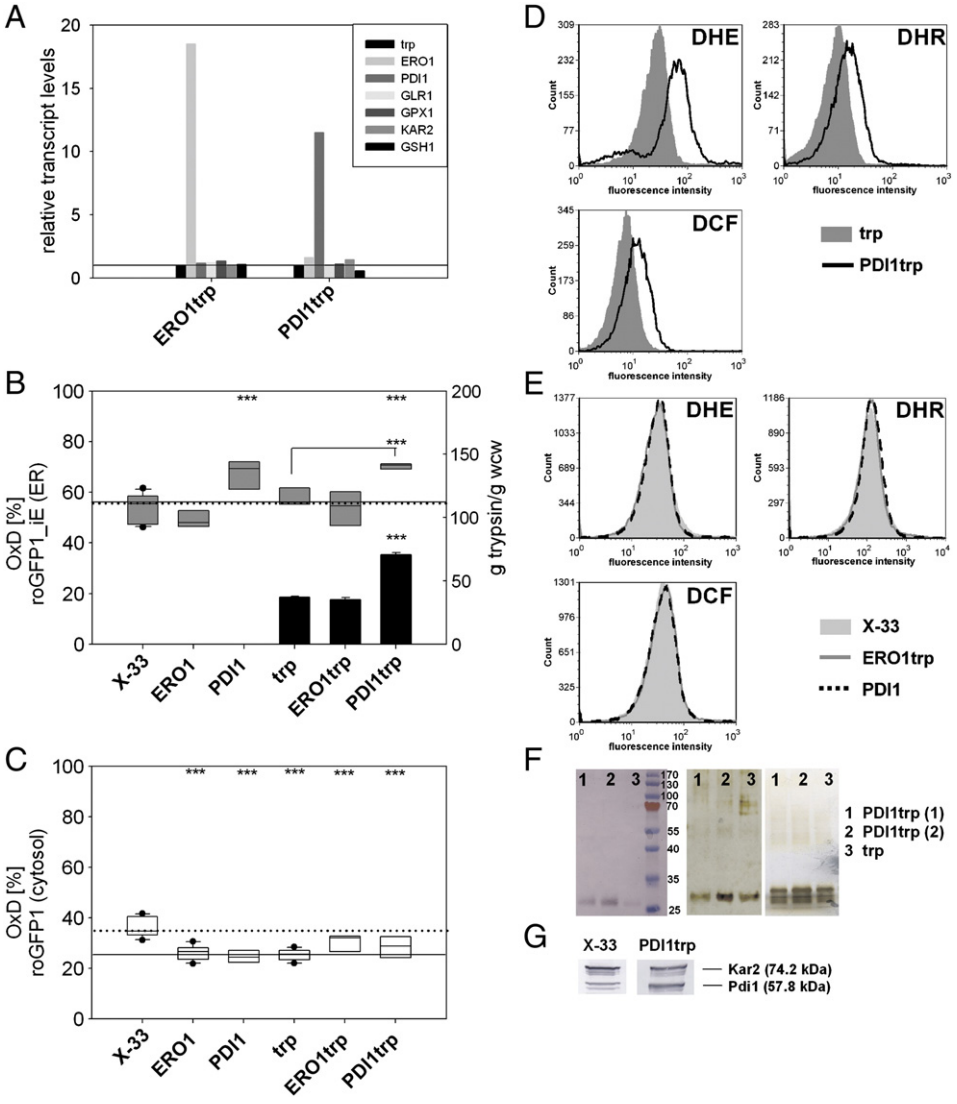

Fig. 4. Overexpression of *PDI1* and *ERO1* leads to reduction of the cytosol, but only *PDI1* causes oxidation of the ER redox state. The wild-type strain X-33 was compared with strains overexpressing *ERO1*, *PDI1*, trp, *ERO1* and trp, or *PDI1* and trp. (A) Transcript levels of the genes trypsinogen, *ERO1*, *PDI1*, *GLR1*, *GPX1*, *KAR2*, and *GSH1* in the trypsinogen-secreting *ERO1* and *PDI1* co-overexpressing strains, compared to wild type. (B) ER redox ratios of the respective strains. ***$p<0.01$, in the upper row indicating a significant difference from X-33, in the next row indicating a significant difference from the trp strain. Secretion levels of trypsinogen are displayed as black bars with significance of differences indicated by ***$p<0.01$. (C) Cytosolic redox ratios of the respective strains. ***$p<0.01$, significant difference from X-33. (D) ROS were measured with the fluorescent dyes DHE, DHR, and DCF in the trp strain and the PDI1trp strain. (E) ROS levels in the wild-type strain (X-33), the ERO1trp strain, and the PDI1 strain. (F) Quality of the secreted porcine trypsinogen (~26 kDa) was analyzed with Western blot (left) and reducing (middle) and nonreducing (right) SDS–PAGE. (G) Western blot analysis of *P. pastoris* cell extracts from the wild-type X-33 and *PDI1*-overexpressing strain with the anti-HDEL antibody.

the wild-type strain (Fig. 6B). Summarizing all the data of this study, the trypsinogen secretion rate correlates with the redox ratio of the ER, but not with that of the cytosol (Figs. 6C and D).

Oxidative protein folding affects intracellular GSSG levels, but not GSH levels

The redox potential of the GSSG/2GSH couple is considered a measure of the cellular redox state, and significant changes in its total amount are often associated with cellular perturbations and stress. To see if glutathione levels are altered during oxidative protein folding, we applied an LC/MS-MS method using hydrophilic interaction chromatography and isotopically labeled internal standards (C. Haberhauer-Troyer et al., manuscript in preparation). Thereby, 2.3 µmol/g wcw GSH and 0.13 µmol/g wcw GSSG were measured in the wild-type strain X-33. In comparison to the wild-type strain, a slight but not significant decrease in the GSH concentration per gram wet cell weight was observed for all deregulated strains except for the *GLR1*-overexpressing strains (Fig. 7A), but no differences among these strains. In contrast, the GSSG levels showed significant variation (Fig. 7B). All deregulated strains, irrespective of trypsinogen production, had a lower intracellular GSSG concentration compared to X-33. The most significant decrease in GSSG levels occurred in the wild-type strain overexpressing *ERO1*, *GLR1*, or *GPX1*. Of the trypsinogen-producing strains GSSG was lowest in strains co-overexpressing *GPX1* or with multiple copies of *PDI1*, but not with single-copy *PDI1* or *ERO1* overexpression.

The supernatants of all strains were analyzed for excreted glutathione. GSH was found in all analyzed samples in an average amount of about 1/10 of the intracellular GSH concentration (Fig. 7C, gray bars). The strain GPX1trp excreted a lower amount of GSH than all other analyzed strains. Regarding the GSSG in the supernatant, concentrations assessed were above the limit of detection, but lower than the limit of quantification. Accordingly, GSSG could not be

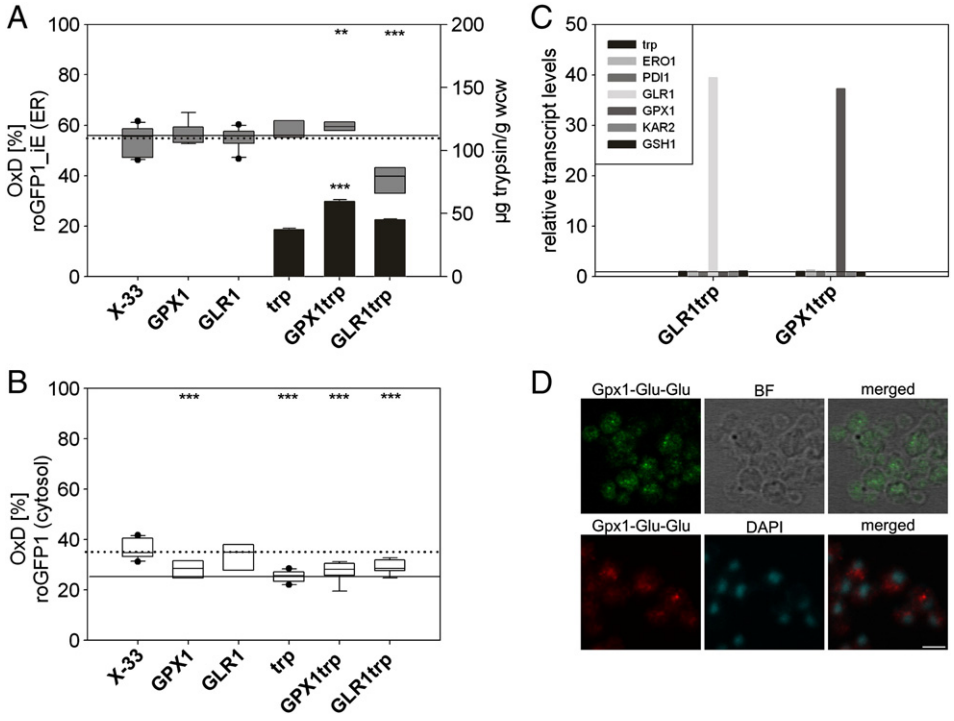

Fig. 5. Co-overproduction of cytosolic glutathione peroxidase increases ER redox state and protein secretion. Comparison of the wild-type strain X-33 with strains overexpressing *GPX1, GLR1,* trypsinogen (trp), *GPX1* and trp, or *GLR1* and trp. (A) ER redox ratios of the respective strains (gray box plots). Statistical significance: $^{**}p<0.05$, $^{***}p<0.01$. The upper row relates to X-33. Secretion levels of trypsinogen are displayed as black bars. (B) Cytosolic redox ratios of the respective strains. $^{***}p<0.01$ compared to X-33. (C) Transcript levels of the genes trypsinogen, *ERO1, PDI1, GLR1, GPX1, KAR2,* and *GSH1* in the trypsinogen-secreting *GLR1*- and *GPX1*-overexpressing strains. (D) Immunofluorescence microscopy of X-33 overexpressing trypsinogen and Gpx1-GluGlu. Top row: Cells were stained with an antibody against GluGlu followed by a secondary fluorescently labeled antibody (Alexa Fluor 488). The fluorescence image was overlaid on a corresponding bright-field image. Bottom row: Cells were double stained with an antibody against GluGlu followed by a secondary fluorescently labeled antibody (Alexa Fluor 555) and DAPI. The two fluorescence images were overlaid. Scale bar, 3 µm.

quantified in the supernatants. However, a quantitative number of the maximum fraction of excreted GSSG could be calculated based on the limit of quantification (~0.007 µmol/g wcw, ~1/10 of the lowest intracellular GSSG concentration).

Oxidative protein folding affects the GSH/GSSG ratio, but does not influence total cellular glutathione levels

Total glutathione concentration was calculated from the measured GSH and GSSG concentrations (Fig. 7C). A slight decrease could be registered for all strains except the *GLR1*-overexpressing strains compared to the wild-type strain, either for intracellular glutathione alone (black) or together with the excreted GSH amount (gray). Correspondingly, transcript levels of *GSH1,* the rate-limiting enzyme in glutathione biosynthesis, were similar in all analyzed strains with the exception of the *PDI1*-overexpressing strain, in which *GSH1* was twofold downregulated (Fig. 4A).

The degree of oxidation, representing the fraction of GSSG within total glutathione, showed more variation among the strains (Fig. 7D). Despite their more reducing cytosol and the lower total glutathione concentration, strains overexpressing *PDI1, ERO1,* and trypsinogen (alone or in combination with *PDI1* or *ERO1*) had ratios similar to those of the wild type. Overexpression of *GPX1* (alone or coexpressed with trypsinogen) led to a significant reduction of the redox buffer glutathione in the cell, as a consequence of the low GSSG levels in these strains. The same is true for *GLR1* overexpression in the wild-type strain. In contrast to the significantly more oxidized redox ratio of the ER, the overall cellular redox state was toward more reducing glutathione ratios in the strains with combined coexpression of *PDI1* and *GPX1* or the multicopy strains of these genes. This leads to the assumption that the cells counterbalance ER oxidation by reduction of cytosolic glutathione.

Discussion

Formation of disulfide bonds is attained through the oxidative protein folding machinery in the ER. It is well established that the ER is a more oxidizing environment than the cytosol, with glutathione playing a major role in controlling the redox state of these organelles. However, there is some controversy as to whether the high level of GSSG in the ER is supporting [31] or rather competing with [32] oxidative protein folding. Induction of the UPR relieves protein folding stress [2,33] and has been demonstrated to cause a reduction of the ER [12]. These facts lead to the assumption that a more reduced ER environment is beneficial for protein folding. On the other hand, the results of this study demonstrate that efficient folding and secretion of proteins correlate with a more oxidizing ER redox potential.

Using a *P. pastoris* strain that is constitutively UPR-induced as a model system, we could verify the reduction of the ER glutathione buffer during ER stress conditions. Apparently, the reductive milieu is needed for disulfide reshuffling of misoxidized proteins or disulfide reduction of terminally misfolded proteins, which is a prerequisite for ER-associated protein degradation (for review, see [34]). During UPR induction, glutathione apparently provides reductive power to the ER and directly reduces Pdi family members, thereby promoting the isomerase/reductase activity of Pdi1 and its homologues. It has been shown in several cases that one main cellular aim is to prevent the release of misfolded proteins [35,36], even at the expense of reduced production rates. This may explain why UPR favors a more “cautious” intracellular environment.

No information on the cytosolic redox state during UPR induction has been reported so far. As chemical induction of ER stress by DTT compromises the redox ratio of the cytosol, the effect of UPR on this compartment can best be studied by endogenous UPR activation. Reduced redox ratios in the cytosol were monitored upon UPR

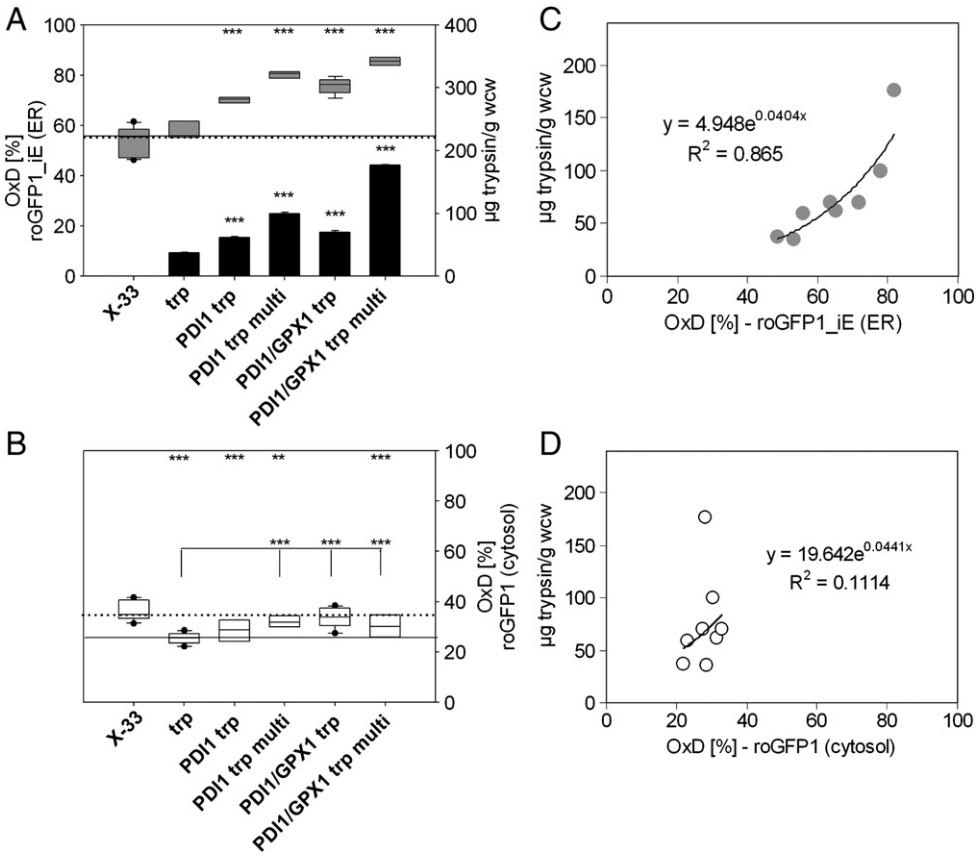

Fig. 6. Combination of *PDI1* and *GPX1* overexpression results in further oxidation of the ER. Comparison of strain X-33 with strains overexpressing trypsinogen and co-overexpressing single and multiple copies of *PDI1* and the combination of *PDI1/GPX1*. (A) ER redox ratios of the respective strains (gray box plots) and secretion levels of trypsinogen (black bars). Statistical significance is indicated as for Fig. 4B. (B) Cytosolic redox ratios of the respective strains. Statistical significance is indicated as for Fig. 4C. The upper row relates to X-33, the lower to trp. (C) Exponential correlation by regression analysis of the ER redox ratio with the amount of secreted trypsinogen. (D) Correlation of the cytosolic redox ratio against the measured amount of secreted trypsinogen.

induction by *HAC1* overexpression or in strains overexpressing high levels of secreted recombinant proteins, e.g., trypsinogen, or antibody fragments. Strong overproduction of mammalian proteins containing disulfide bonds presents a challenge for the yeast protein folding machinery [33]; therefore these strains may serve as models as their intracellular redox environment probably reflects the conditions in highly productive mammalian cells such as pancreas or plasma cells.

Without causing UPR induction, secretion of a disulfide-rich model protein did not influence ER redox state, but led to a reduction of the cytosol once again. A similar reduction of the cytosol was observed in strains overproducing the two ER-resident members of the oxidative protein folding pathway, Ero1 and Pdi1, but not for overproduction of the cytosolic enzyme Glr1 or recombinant cytosolic proteins. Reduction of the cytosol apparently is a specific reaction to enhanced oxidative protein folding within the ER, whereas ER reduction is a response to regulation by UPR.

In contrast to UPR-induced cells, we could demonstrate that the ER can be further oxidized by overexpression of *PDI1* and/or *GPX1*, single or multicopy, which also correlates with the amount of secreted recombinant trypsinogen. Correct disulfide bonding and folding of trypsinogen are assumed as quantification is based on trypsin activity. In contrast to results obtained in mammalian cells [37,38], we did not observe the formation of aggregates or the secretion of misfolded proteins in this study (Fig. 4F). This may be because the folding machinery is not at its limit in the single-copy trypsinogen strain or may indicate a stringent ER quality control mechanism and efficient degradation of misfolded proteins in *P. pastoris*, as recently reported in [39]. As a positive effect of *PDI1* overexpression has been reported for a number of secreted proteins in *P. pastoris* and other eukaryotes [33,40] one can assume that higher secretion rates generally correlate with a more oxidized ER. This is in line with a recent report by Lappi and Ruddock [31], who reclaim the role of glutathione and the oxidizing conditions in the ER as major players in oxidative protein folding.

Deregulation of Ero1 did not highly influence the ER redox state in this study. As feedback regulation for this protein has been reported (reviewed in [41]), one can assume that the excess Ero1 protein was in the inactive state without its substrate (reduced Pdi1). In contrast, Pdi1, if present more abundantly, seems to act more on its targets, leading to a more oxidized ER environment, and may also activate Ero1. Whereas mammalian PDI1 is predominantly present in its reduced state in various mammalian cell lines [42], *S. cerevisiae* Pdi1 is mainly found in its oxidized form [43–46]. Though we did not analyze the *P. pastoris* Pdi1 redox state because of a lack of a specific antibody, our redox results indicate that *P. pastoris* Pdi1 is also predominantly present in its oxidized state, ready to act as an oxidase, and that Pdi1 activity in vivo leads to a net production of oxidized species [47]. This is even more emphasized in a strain co-overexpressing trypsinogen and Pdi1, in which Pdi1 can act on a more abundant substrate leading to further oxidation of the ER. *ERO1* co-overexpression, on the other side, does not lead to a significant change of the ER redox ratio and does not seem to be the rate-limiting factor for oxidative protein folding in *P. pastoris*. Correspondingly, overexpression of Pdi1 in the trypsinogen-producing strain led to the formation of ROS, in contrast to the *ERO1* co-overexpressing strain. Similar results

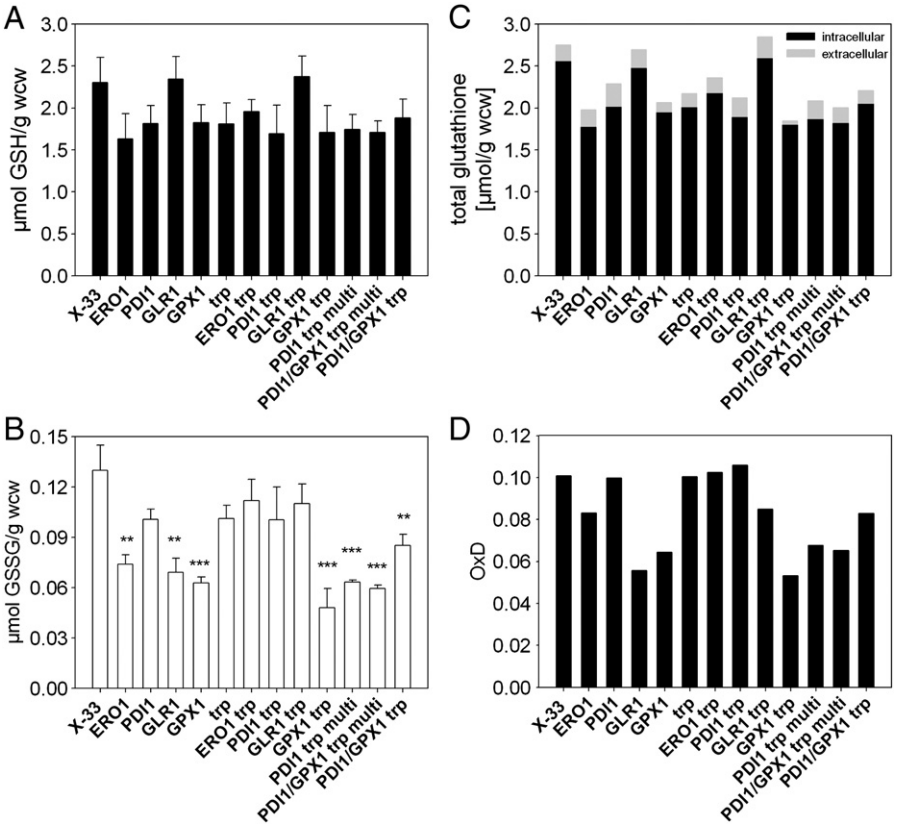

Fig. 7. Comparison of intra- and extracellular glutathione (GSH) and glutathione disulfide (GSSG) levels of various strains. (A) Intracellular GSH concentrations (µmol GSH per g wcw). Differences were not statistically significant ($p > 0.1$). (B) Intracellular GSSG concentrations (µmol GSSG per g wcw). *** $p < 0.01$; ** $p < 0.05$. (C) Total glutathione (tGSH) concentration was determined using the equation tGSH = [GSH] + 2[GSSG]. (D) Degree of oxidation (OxD) calculated as OxD = 2[GSSG]/([GSH] + 2[GSSG]). OxD represents the fraction of tGSH present as GSSG.

were observed when co-overexpressing *S. cerevisiae PDI1* or *ERO1* in 2F5 Fab-secreting *P. pastoris* strains (own unpublished data), thus pointing to similar regulatory mechanisms of the proteins from both yeast species.

It is noteworthy that overexpression of *GPX1*, which we proved to be localized in the cytosol and not the ER, causes oxidation of the ER glutathione pool when co-overexpressed with trypsinogen. To our knowledge this is the first report showing the involvement of cytosolic glutathione peroxidase in the oxidative protein folding pathway. On the other hand, an ER-resident peroxidase could not be identified in the genome of yeast so far.

A striking observation of this study is that overproduction of disulfide bond-rich proteins or components of the ER-resident oxidative folding machinery leads to a reduction of the cytosol. However, this effect can be attributed neither to specific excretion of GSSG to the cell exterior nor to increased levels of glutathione biosynthesis. Moreover, the cytosolic enzymes Glr1 and Gpx1 involved in glutathione homeostasis strongly influenced the ER redox conditions when co-overexpressed with the disulfide-rich secretory protein trypsinogen.

Our results thereby confirm the hypothesis of intercompartmental redox homeostasis between ER and cytosol introduced by Molteni et al. [38]. However, in contrast to their results in HeLa cells, we did not observe increased levels of glutathione or induction of glutathione biosynthesis upon overexpression of *PDI1* or *ERO1*, but a specific shift of the redox milieu of the cytosol. The simplest way of redox exchange between ER and cytosol would be the transport of glutathione from the ER to the cytosol or vice versa. Both transport of GSH and GSSG via the ER membrane have been discussed [10], GSH being probably the preferential transported form [48]. However, this cannot quantitatively lead to the observed reduction of the cytosol; in other words, either potential GSSG transport from cytosol to ER or electron transport via the membrane must be involved, in addition to a reduction of GSSG to GSH in the cytoplasm (by means other than Glr1). Alternatively, molecular sensors may exist that monitor the redox conditions in the ER lumen and transmit the signal to the cytosolic side of the ER membrane, as reported for redox sensing by Ca^{2+} signaling in mammalian cells. Other possible means of signaling may include ROS such as H_2O_2 (reviewed in [49,50]). These may allow independent oxidation of GSH in the ER through the action of Pdi1 (as observed in *PDI1* and *GPX1* co-overexpressing strains) and reduction of glutathione in the cytoplasm. It remains to be analyzed if Ca^{2+} release from the ER in yeast is also regulated by Ero1, as recently reported for mammalian cells [51]. Balancing the redox milieu in living cells seems rather complex; therefore further research focusing on the analysis of the redox cross talk between the ER and the cytoplasm is required.

Conclusions

Induction of UPR triggers a complex regulatory pattern, which mainly aims at refolding or degradation of misfolded proteins within the ER, but is distinct from the response to folding of secretory proteins without ER stress. Deregulation of redox active enzymes points towards a correlation of ER oxidation state and secretion efficiency. Our data demonstrate clearly that protein folding and ER stress have a severe impact on the cytosolic redox balance which may be a major factor during development of folding related diseases.

Acknowledgments

The authors thank Dr. S. James Remington (University of Oregon, Eugene, OR, USA) for providing the roGFP1 and roGFP1_iE genes. The authors also thank Gabi Wilt for help with real-time PCR and Justyna Nocon for help with ROS analysis. Thanks to Martin Pfeffer and Johannes Grillari for critical reading of the manuscript. Special thanks to Benjamin Glick (University of Chicago, USA) for his kind and engaged introduction into Pichia microscopy. C.R. is funded by the doctoral program "BioToP–Biomolecular Technology of Proteins" (Austrian Science Fund, FWF Project W1224). Further support by the Federal Ministry of Economy, Family, and Youth; the Federal Ministry of Traffic, Innovation, and Technology; the Styrian Business Promotion Agency SFG; the Standortagentur Tirol; and ZIT–Technology Agency of the City of Vienna through the COMET-Funding Program managed by the Austrian Research Promotion Agency FFG is acknowledged. Finally, we thank the University of Natural Resources and Life Sciences Vienna–VIBT Imaging Center for access and expertise with the Leica DMI 6000 fluorescence microscope and the DMI 6000 SP5 confocal laser scanning microscope.

Appendix A. Supplementary material

Supplementary data associated with this article can be found in the online version at doi:10.1016/j.freeradbiomed.2012.02.048.

References

[1] Goeckeler, J. L.; Brodsky, J. L. Molecular chaperones and substrate ubiquitination control the efficiency of endoplasmic reticulum-associated degradation. *Diabetes Obes. Metab.* **12** (Suppl. 2)**:**32–38; 2010.
[2] Malhotra, J. D.; Kaufman, R. J. The endoplasmic reticulum and the unfolded protein response. *Semin. Cell Dev. Biol.* **18:**716–731; 2007.
[3] Yoshida, H. ER stress and diseases. *FEBS J.* **274:**630–658; 2007.
[4] Townsend, D. M.; Tew, K. D.; Tapiero, H. The importance of glutathione in human disease. *Biomed. Pharmacother.* **57:**145–155; 2003.
[5] Vené, R.; Delfino, L.; Castellani, P.; Balza, E.; Bertolotti, M.; Sitia, R.; Rubartelli, A. Redox remodeling allows and controls B-cell activation and differentiation. *Antioxid. Redox Signal.* **13:**1145–1155; 2010.
[6] Cenci, S.; Sitia, R. Managing and exploiting stress in the antibody factory. *FEBS Lett.* **581:**3652–3657; 2007.
[7] Tu, B. P.; Ho-Schleyer, S. C.; Travers, K. J.; Weissman, J. S. Biochemical basis of oxidative protein folding in the endoplasmic reticulum. *Science* **290:**1571–1574; 2000.
[8] Penninckx, M. J. An overview on glutathione in Saccharomyces versus non-conventional yeasts. *FEMS Yeast Res.* **2:**295–305; 2002.
[9] Lopez-Mirabal, H. R.; Winther, J. R. Redox characteristics of the eukaryotic cytosol. *Biochim. Biophys. Acta* **1783:**629–640; 2008.
[10] Hwang, C.; Sinskey, A.; Lodish, H. Oxidized redox state of glutathione in the endoplasmic reticulum. *Science* **257:**1496–1502; 1992.
[11] Dixon, B. M.; Heath, S. H.; Kim, R.; Suh, J. H.; Hagen, T. M. Assessment of endoplasmic reticulum glutathione redox status is confounded by extensive ex vivo oxidation. *Antioxid. Redox Signal.* **10:**963–972; 2008.
[12] Merksamer, P.; Trusina, A.; Papa, F. Real-time redox measurements during endoplasmic reticulum stress reveal interlinked protein folding functions. *Cell* **135:** 933–947; 2008.
[13] Delic, M.; Mattanovich, D.; Gasser, B. Monitoring intracellular redox conditions in the endoplasmic reticulum of living yeasts. *FEMS Microbiol. Lett.* **306:**61–66; 2010.
[14] Kohno, K. Stress-sensing mechanisms in the unfolded protein response: similarities and differences between yeast and mammals. *J. Biochem.* **147:**27–33; 2010.
[15] Papanikou, E.; Glick, B. S. The yeast Golgi apparatus: insights and mysteries. *FEBS Lett.* **583:**3746–3751; 2009.
[16] Bánhegyi, G.; Baumeister, P.; Benedetti, A.; Dong, D.; Fu, Y.; Lee, A. S.; Li, J.; Mao, C.; Margittai, E.; Ni, M.; Paschen, W.; Piccirella, S.; Senesi, S.; Sitia, R.; Wang, M.; Yang, W. Endoplasmic reticulum stress. *Ann. N. Y. Acad. Sci.* **1113:**58–71; 2007.
[17] Lohman, J.; Remington, S. Development of a family of redox-sensitive green fluorescent protein indicators for use in relatively oxidizing subcellular environments. *Biochemistry* **47:**8678–8688; 2008.
[18] van Lith, M.; Tiwari, S.; Pediani, J.; Milligan, G.; Bulleid, N. J. Real-time monitoring of redox changes in the mammalian endoplasmic reticulum. *J. Cell Sci.* **124:**2349–2356; 2011.
[19] Stadlmayr, G.; Mecklenbräuker, A.; Rothmüller, M.; Maurer, M.; Sauer, M.; Mattanovich, D.; Gasser, B. Identification and characterisation of novel Pichia pastoris promoters for heterologous protein production. *J. Biotechnol.* **150:**519–529; 2010.
[20] Marx, H.; Mattanovich, D.; Sauer, M. Overexpression of the riboflavin biosynthetic pathway in Pichia pastoris. *Microb. Cell Fact.* **7:**23; 2008.
[21] Grussenmeyer, T.; Scheidtmann, K. H.; Hutchinson, M. A.; Eckhart, W.; Walter, G. Complexes of polyoma virus medium T antigen and cellular proteins. *Proc. Natl. Acad. Sci. U. S. A.* **82:**7952–7954; 1985.
[22] Meyer, A. J.; Dick, T. P. Fluorescent protein-based redox probes. *Antioxid. Redox Signal.* **13:**621–650; 2010.
[23] Hohenblum, H.; Borth, N.; Mattanovich, D. Assessing viability and cell-associated product of recombinant protein producing Pichia pastoris with flow cytometry. *J. Biotechnol.* **102:**281–290; 2003.
[24] Graf, A.; Gasser, B.; Dragosits, M.; Sauer, M.; Leparc, G.; Tuechler, T.; Kreil, D.; Mattanovich, D. Novel insights into the unfolded protein response using Pichia pastoris specific DNA microarrays. *BMC Genomics* **9:**390; 2008.
[25] Haynes, C. M.; Titus, E. A.; Cooper, A. A. Degradation of misfolded proteins prevents ER-derived oxidative stress and cell death. *Mol. Cell* **15:**767–776; 2004.
[26] Tan, S. X.; Teo, M.; Lam, Y. T.; Dawes, I. W.; Perrone, G. G. Cu, Zn superoxide dismutase and NADP(H) homeostasis are required for tolerance of endoplasmic reticulum stress in Saccharomyces cerevisiae. *Mol. Biol. Cell* **20:**1493–1508; 2009.
[27] Sauer, B. Functional expression of the cre-lox site-specific recombination system in the yeast Saccharomyces cerevisiae. *Mol. Cell. Biol.* **7:**2087–2096; 1987.
[28] Yano, T.; Takigami, E.; Yurimoto, H.; Sakai, Y. Yap1-regulated glutathione redox system curtails accumulation of formaldehyde and reactive oxygen species in methanol metabolism of Pichia pastoris. *Eukaryot. Cell* **8:**540–549; 2009.
[29] Mattanovich, D.; Graf, A.; Stadlmann, J.; Dragosits, M.; Redl, A.; Maurer, M.; Kleinheinz, M.; Sauer, M.; Altmann, F.; Gasser, B. Genome, secretome and glucose transport highlight unique features of the protein production host Pichia pastoris. *Microb. Cell Fact.* **8:**29; 2009.
[30] Ukai, Y.; Kishimoto, T.; Ohdate, T.; Izawa, S.; Inoue, Y. Glutathione peroxidase 2 in Saccharomyces cerevisiae is distributed in mitochondria and involved in sporulation. *Biochem. Biophys. Res. Commun.* **411:**580–585; 2011.
[31] Lappi, A. K.; Ruddock, L. W. Reexamination of the role of interplay between glutathione and protein disulfide isomerase. *J. Mol. Biol.* **409:**238–249; 2011.
[32] Cuozzo, J. W.; Kaiser, C. A. Competition between glutathione and protein thiols for disulphide-bond formation. *Nat. Cell Biol.* **1:**130–135; 1999.
[33] Gasser, B.; Saloheimo, M.; Rinas, U.; Dragosits, M.; Rodríguez-Carmona, E.; Baumann, K.; Giuliani, M.; Parrilli, E.; Branduardi, P.; Lang, C.; Porro, D.; Ferrer, P.; Tutino, M.; Mattanovich, D.; Villaverde, A. Protein folding and conformational stress in microbial cells producing recombinant proteins: a host comparative overview. *Microb. Cell Fact.* **7:**11; 2008.
[34] Fassio, A.; Sitia, R. Formation, isomerisation and reduction of disulphide bonds during protein quality control in the endoplasmic reticulum. *Histochem. Cell Biol.* **117:**151–157; 2002.
[35] Hoseki, J.; Ushioda, R.; Nagata, K. Mechanism and components of endoplasmic reticulum-associated degradation. *J. Biochem.* **147:**19–25; 2010.
[36] Vembar, S. S.; Brodsky, J. L. One step at a time: endoplasmic reticulum-associated degradation. *Nat. Rev. Mol. Cell Biol.* **9:**944–957; 2008.
[37] Chakravarthi, S.; Bulleid, N. J. Glutathione is required to regulate the formation of native disulfide bonds within proteins entering the secretory pathway. *J. Biol. Chem.* **279:**39872–39879; 2004.
[38] Molteni, S. N.; Fassio, A.; Ciriolo, M. R.; Filomeni, G.; Pasqualetto, E.; Fagioli, C.; Sitia, R. Glutathione limits Ero1-dependent oxidation in the endoplasmic reticulum. *J. Biol. Chem.* **279:**32667–32673; 2004.
[39] Pfeffer, M.; Maurer, M.; Kollensperger, G.; Hann, S.; Graf, A. B.; Mattanovich, D. Modeling and measuring intracellular fluxes of secreted recombinant protein in Pichia pastoris with a novel 34S labeling procedure. *Microb. Cell Fact.* **10:**47; 2011.
[40] Davis, R.; Schooley, K.; Rasmussen, B.; Thomas, J.; Reddy, P. Effect of PDI overexpression on recombinant protein secretion in CHO cells. *Biotechnol. Prog.* **16:**736–743; 2000.
[41] Tavender, T. J.; Bulleid, N. J. Molecular mechanisms regulating oxidative activity of the Ero1 family in the endoplasmic reticulum. *Antioxid. Redox Signal.* **13:**1177–1187; 2010.
[42] Mezghrani, A.; Fassio, A.; Benham, A.; Simmen, T.; Braakman, I.; Sitia, R. Manipulation of oxidative protein folding and PDI redox state in mammalian cells. *EMBO J.* **20:**6288–6296; 2001.
[43] Frand, A. R.; Kaiser, C. A. Ero1p oxidizes protein disulfide isomerase in a pathway for disulfide bond formation in the endoplasmic reticulum. *Mol. Cell* **4:** 469–477; 1999.
[44] Vitu, E.; Kim, S.; Sevier, C. S.; Lutzky, O.; Heldman, N.; Bentzur, M.; Unger, T.; Yona, M.; Kaiser, C. A.; Fass, D. Oxidative activity of yeast Ero1p on protein disulfide isomerase and related oxidoreductases of the endoplasmic reticulum. *J. Biol. Chem.* **285:**18155–18165; 2010.
[45] Tu, B. P.; Weissman, J. S. Oxidative protein folding in eukaryotes: mechanisms and consequences. *J. Cell Biol.* **164:**341–346; 2004.
[46] Sevier, C. S.; Qu, H.; Heldman, N.; Gross, E.; Fass, D.; Kaiser, C. A. Modulation of cellular disulfide-bond formation and the ER redox environment by feedback regulation of Ero1. *Cell* **129:**333–344; 2007.
[47] Hatahet, F.; Ruddock, L. W. Protein disulfide isomerase: a critical evaluation of its function in disulfide bond formation. *Antioxid. Redox Signal.* **11:**2807–2850; 2009.
[48] Bánhegyi, G.; Lusini, L.; Puskás, F.; Rossi, R.; Fulceri, R.; Braun, L.; Mile, V.; di Simplicio, P.; Mandl, J.; Benedetti, A. Preferential transport of glutathione versus glutathione disulfide in rat liver microsomal vesicles. *J. Biol. Chem.* **274:**12213–12216; 1999.
[49] Csala, M.; Margittai, E.; Banhegyi, G. Redox control of endoplasmic reticulum function. *Antioxid. Redox Signal.* **13:**77–108; 2010.
[50] Margittai, E.; Sitia, R. Oxidative protein folding in the secretory pathway and redox signaling across compartments and cells. *Traffic* **12:**1–8; 2011.
[51] Anelli, T.; Bergamelli, L.; Margittai, E.; Rimessi, A.; Fagioli, C.; Malgaroli, A.; Pinton, P.; Ripamonti, M.; Rizzuto, R.; Sitia, R. Ero1α regulates Ca^{2+} fluxes at the endoplasmic reticulum–mitochondria interface (MAM). *Antioxid. Redox Signal.* **16:**1077–1087; 2012.

[52] Gasser, B.; Sauer, M.; Maurer, M.; Stadlmayr, G.; Mattanovich, D. Transcriptomics-based identification of novel factors enhancing heterologous protein secretion in yeasts. *Appl. Environ. Microbiol.* **73:**6499–6507; 2007.
[53] Baumann, K.; Maurer, M.; Dragosits, M.; Cos, O.; Ferrer, P.; Mattanovich, D. Hypoxic fed-batch cultivation of Pichia pastoris increases specific and volumetric productivity of recombinant proteins. *Biotechnol. Bioeng.* **100:**177–183; 2008.
[54] Kilmartin, J. V.; Adams, A. E. Structural rearrangements of tubulin and actin during the cell cycle of the yeast Saccharomyces. J. Cell Biol. **98:**922–933; 1984.
[55] Rossanese, O. W.; Sonderholm, J.; Bevis, B. J.; Sears, I. B.; O'Connor, J.; Williamson, E. K.; Glick, B. S. Golgi structure correlates with transitional endoplasmic reticulum organization in *Pichia pastoris* and *Saccharomyces cerevisiae*. *J. Cell Biol.* **145:**69–81; 1999.